Universality in the spectral and eigenfunction properties of random networks

J. A. Méndez-Bermúdez* and A. Alcazar-López
Instituto de Física, Benemérita Universidad Autónoma de Puebla, Apartado Postal J-48, Puebla 72570, Mexico

A. J. Martínez-Mendoza
Instituto de Física, Benemérita Universidad Autónoma de Puebla, Apartado Postal J-48, Puebla 72570, Mexico and Elméleti Fizika Tanszék, Fizikai Intézet, Budapesti Műszaki és Gazdaságtudományi Egyetem, H-1521 Budapest, Hungary

Francisco A. Rodrigues
Departamento de Matemática Aplicada e Estatística, Instituto de Ciências Matemáticas e de Computação, Universidade de São Paulo, Caixa Postal 668,13560-970 São Carlos, São Paulo, Brazil

Thomas K. DM. Peron
Instituto de Física de São Carlos, Universidade de São Paulo, CP 369, 13560-970, São Carlos, São Paulo, Brazil
(Received 29 August 2014; published 13 March 2015)

By the use of extensive numerical simulations, we show that the nearest-neighbor energy-level spacing distribution $P(s)$ and the entropic eigenfunction localization length of the adjacency matrices of Erdős-Rényi (ER) fully random networks are universal for fixed average degree $\xi \equiv \alpha N$ (α and N being the average network connectivity and the network size, respectively). We also demonstrate that the Brody distribution characterizes well $P(s)$ in the transition from $\alpha = 0$, when the vertices in the network are isolated, to $\alpha = 1$, when the network is fully connected. Moreover, we explore the validity of our findings when relaxing the randomness of our network model and show that, in contrast to standard ER networks, ER networks with diagonal disorder also show universality. Finally, we also discuss the spectral and eigenfunction properties of small-world networks.

DOI: 10.1103/PhysRevE.91.032122 PACS number(s): 64.60.−i, 05.45.Pq, 89.75.Hc

I. INTRODUCTION

Networks have been used to represent the organization of complex systems such as social networks, the Internet, and ecosystems [1,2]. Depending on the application, vertices and edges have different meanings [1,3]. For example, in condensed matter physics, vertices and edges of the ordered network known as Anderson's tight-binding model are the sites and hopping integrals, respectively [4]. Networks can be deterministic, fractal, or random [5]. Deterministic and fractal networks are constructed following specific rules, whereas for random networks a set of parameters take fixed values but the network itself has a random organization. In the latter case it is meaningless to study a single random network; instead a statistical analysis of an ensemble of networks with the same average properties should be performed. Several models of random networks have been introduced [3,6], including Erdős-Rényi (ER) random graphs, the scale-free network model of Barabási and Albert, and the small-world networks of Watts and Strogatz. These models are considered to reproduce the organization of real-world networks, such as the Internet, power grids, and social and biological networks [1,3,6]. Although random graphs fail in predicting most of the properties observed in real-world networks, such as power-law degree distributions and nonvanishing clustering coefficient [6], such graphs have been thoroughly studied theoretically (e.g., [7]). Indeed, many results, such as the emergence of percolation, can be obtained analytically in ER networks [3,7].

Here we consider the ER random graph model, which was introduced by Solomonoff and Rapoport [8] and thoroughly studied later by Erdős and Rényi [9,10]. This model is also known as uncorrelated random graph model. Erdős-Rényi networks are constructed by starting with N isolated vertices and afterward each pair of vertices is connected according to a probability α. This process is a type of N^2-realization Bernoulli process with probability of success α. Therefore, the number of connections follows a binomial distribution. Nevertheless, most realizations of this model take into account large values of N and small values of α. In this way, the degree distribution tends to a Poisson distribution due to the law of rare events.

Independently of the field, classification, or application, a commonly accepted mathematical representation of a network is the adjacency matrix. The adjacency matrix $\mathbf{A}$ of a simple network, i.e., a network having no multiple edges or self-edges, is the matrix with elements A_{ij} defined as [3]

$$A_{ij} = \begin{cases} 1 & \text{if there is an edge between vertices } i \text{ and } j \\ 0 & \text{otherwise.} \end{cases} \quad (1)$$

This prescription produces $N \times N$ symmetric sparse matrices with zero diagonal elements, where N is the number of vertices of the corresponding network. The sparsity of $\mathbf{A}$ is quantified by the parameter α, which is the fraction of nonvanishing off-diagonal adjacency matrix elements. Vertices are isolated when $\alpha = 0$, whereas the network is fully connected for $\alpha = 1$. Once the adjacency matrix of a network is constructed, it is quite natural to ask about its spectral and eigenfunction properties, which is the main subject of this paper. As commonly used, we refer to the spectral and eigenfunction properties

*jmendezb@ifuap.buap.mx

of the adjacency matrix as the spectral and eigenfunction properties of the respective network.

Moreover, there is a one-to-one correspondence between the adjacency matrix **A** and the Hamiltonian matrix **H** of a ξ-dimensional solid, described by Anderson's tight-binding model [4] with zero on-site potentials ($H_{ii} = 0$) and constant hopping integrals ($H_{ij} = 1$). Here ξ is proportional to the average nonzero off-diagonal adjacency matrix elements per matrix row and therefore may be regarded as the effective dimension of the network represented by **A**, as discussed in Ref. [11] from a random matrix theory (RMT) point of view. This correspondence enables the direct application of studies originally motivated by physical systems, represented by Hamiltonian sparse random matrices, to complex networks. In the network literature, ξ is known as the average degree of a network. Moreover, notice that

$$\xi = \alpha N, \tag{2}$$

where ξ is defined as the mean number of nonzero elements per matrix row. From a mathematical-physicist point of view, in the frame of RMT, Rodgers and Bray [12] proposed an ensemble of sparse random matrices characterized by the connectivity ξ. Since then, several papers have been devoted to analytical and numerical studies of sparse symmetric random matrices (see, for example, [11–25]).

Among the most relevant results of these studies we can mention that (i) in the very sparse limit $\xi \to 1$, the density of states was found to deviate from the Wigner semicircle law with the appearance of singularities, around and at the band center, and tails beyond the semicircle [12–21]; (ii) a delocalization transition was found at $\xi \approx 1.4$ [14–16,22]; (iii) the nearest-neighbor energy-level spacing distribution $P(s)$ was found to evolve from the Poisson to the Gaussian orthogonal ensemble (GOE) predictions for increasing ξ [11,14,16] (the same transition was reported for the number variance in Ref. [11]). More recently, the first eigenvalue-eigenfunction problem was also addressed in Ref. [23]. Also, non-Hermitian sparse matrices were discussed in Ref. [24].

It is relevant to emphasize that the RMT model of sparse matrices introduced by Rodgers and Bray [12] is equivalent to adjacency matrices of ER-type networks. In fact, motivated by this equivalency and based on the ER model, here we study spectral and eigenfunction properties of the following random network model: Starting with the standard ER network, we add to it self-edges and further consider all edges to have random strengths.[1] We call this model the ER fully random network model. The sparsity α is defined as the fraction of $N(N-1)/2$ independent nonvanishing off-diagonal adjacency matrix elements. Then, as in the standard ER model, the ER fully random network model is characterized only by the parameters N and α. However, the corresponding adjacency matrices come from the ensemble of $N \times N$ sparse real symmetric matrices whose nonvanishing elements are statistically independent random variables drawn from a normal distribution with zero mean $\langle A_{ij} \rangle = 0$ and variance $\langle |A_{ij}|^2 \rangle = (1 + \delta_{ij})/2$. According to this definition, a diagonal random matrix is obtained for $\alpha = 0$ (Poisson case), whereas the GOE is recovered when $\alpha = 1$.

Our motivation to study spectral and eigenfunction properties of the ER fully random network model is twofold. On the one hand, Jackson *et al.* [11] showed that the disorder parameter ξ fixes some spectral features of sparse random matrices equivalent to the adjacency matrices we study here. Moreover, it is also known that the average degree ξ fixes some properties of random graphs [26]. On the other hand, there is a large number of papers studying spectral and eigenfunction properties of complex networks [27–56]. However, most of those studies focus on networks with specific combinations of N and α. For instance, Refs. [32–37,49] investigated random networks using concepts of RMT, centering the attention on networks with fixed N and α, even when more sophisticated topological properties are included in the network models, such as the nonvanishing clustering coefficient [32] and modular structure [36]. Moreover, Palla and Vallay [27] investigated spectral properties of standard ER networks close to the critical point of percolation, restricting the analysis to values of $1 < \xi < 2.4$.

Then we realized that the universality (in the sense of identifying relevant network parameters) of the spectral and eigenfunction properties of ER-type random networks has not been completely explored yet. Thus, in this paper we undertake this task, having as a reference RMT models and predictions. Furthermore, our investigations generalize previous results in the literature by not restricting our analysis to a specific combination of network parameters or even to a specific network model.

In the next section we analyze $P(s)$, i.e., the nearest-neighbor energy-level spacing distribution, the average Shannon entropy $\langle S \rangle$, and the entropic eigenfunction localization length ℓ_N for the ER fully random network model as a function of the connectivity α. It is well known that $P(s)$, the probability distribution function of the spacings between adjacent eigenvalues, plays a prominent role in the description of disordered and quantized classically chaotic systems [57,58]. We show that $P(s)$, $\langle S \rangle$, and ℓ_N are all invariant for fixed average degree ξ. In addition, we show that the Brody distribution fits well $P(s)$ in the transition from isolated to fully connected networks. By noticing that the ER fully random network model displays maximal disorder, in Sec. III we explore the validity of our findings when relaxing the randomness of this network model. Therefore, we show that the ER network model with diagonal disorder (i.e., ER model including random strength self-edges) also exhibits universality for fixed ξ. We also apply our approach to a different random network model, so in Sec. IV we comment on the spectral and eigenfunction properties of small-world random networks. Our conclusions are summarized in Sec. V.

II. ERDŐS-RÉNYI FULLY RANDOM NETWORKS

In the following we use exact numerical diagonalization to obtain the eigenvalues E^m and eigenfunctions Ψ^m ($m = 1, \ldots, N$) of the adjacency matrices of large ensembles of random networks characterized by N and α.

[1] We justify the addition of random strengths to edges by recognizing that in real-world networks connections and interactions are in general nonconstant.

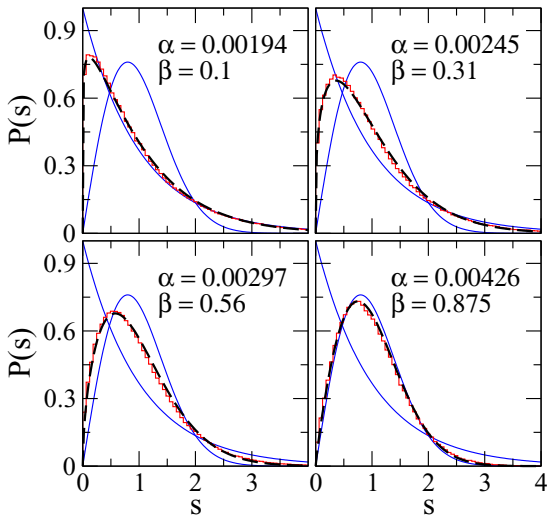

FIG. 1. (Color online) Nearest-neighbor energy-level spacing distribution $P(s)$ for ER fully random networks of size $N = 1000$ and different connectivity values α (red histograms). Blue lines correspond to Poisson and Wigner-Dyson distribution functions given by Eqs. (3) and (4), respectively. Black dashed lines are fittings of the histograms with the Brody distribution of Eq. (5), where the fitted values of β are given in the corresponding panels. The histograms were computed from 5×10^5 unfolded spacings.

A. Nearest-neighbor energy-level spacing distribution

Figure 1 presents the nearest-neighbor energy-level spacing distribution $P(s)$ for the adjacency matrices of ER fully random networks of size $N = 1000$ and different connectivity values α. The histograms were constructed by the use of the 500 unfolded spacings [57] $s_m = (E^{m+1} - E^m)/\Delta$ around the band center of 10^3 random matrices. Here Δ is the mean level spacing computed for each adjacency matrix as the slope of the curve E^m vs m around the band center. When other network sizes are considered, we always construct $P(s)$ from half of the total eigenvalues around the band center, where the density of states is approximately constant.

For $\alpha = 0$, i.e., when the vertices in the network are isolated, the corresponding adjacency matrices are diagonal and $P(s)$ follows the exponential distribution

$$P(s) = \exp(-s), \tag{3}$$

better known in RMT as the Poisson distribution or the spacing rule for random levels [57]. In the opposite limit $\alpha = 1$, when the network is fully connected, the adjacency matrices become members of the GOE (full real symmetric random matrices) and $P(s)$ closely follows the Wigner-Dyson distribution[2] [57]

$$P(s) = \frac{\pi}{2} s \exp\left(-\frac{\pi}{4} s^2\right). \tag{4}$$

Then, by increasing α from zero to one, the shape of $P(s)$ should evolve from the Poisson to the Wigner-Dyson distribution. This transition, partially observed for our random network model in Refs. [11,14] from a pure RMT point of view, is well depicted in Fig. 1, where we also plot Eqs. (3) and (4) as reference. In fact, it is interesting to mention that for relatively small values of α the limiting GOE statistics is recovered. The transition from Poisson to Wigner-Dyson in the spectral statistics has also been reported for adjacency matrices corresponding to other complex network models in Refs. [29–36].

Here, in order to characterize the shape of $P(s)$ for our random networks we use the Brody distribution [59,60], which was originally derived to provide an interpolation expression for $P(s)$ in the transition from a Poisson to a Wigner-Dyson distribution by making the ansatz $P(s) = c_1 s^\beta \exp(-c_2 s^{\beta+1})$ (with $c_{1,2}$ depending on β). Then, after proper normalization the Brody distribution reads [59,60]

$$P(s) = (\beta + 1) a_\beta s^\beta \exp(-a_\beta s^{\beta+1}), \tag{5}$$

where $a_\beta = [\Gamma(\beta + 2/\beta + 1)]^{\beta+1}$, $\Gamma(\cdot)$ is the Gamma function, and β, known as the Brody parameter, takes values in the range $[0,1]$. Here $\beta = 0$ and 1 reproduce the Poisson and Wigner-Dyson distributions, respectively. We remark that, even though the Brody distribution has been extensively used to characterize $P(s)$ having fractional power-law level repulsion [61], it has been obtained through a purely phenomenological approach and the Brody parameter has no decisive physical meaning [62] but serves as a measure for the degree of mixing between the Poisson and GOE statistics. In particular, as we show below, the Brody parameter will allows us to identify the onset of the delocalization transition and the onset of the GOE limit in our random network models.

Black dashed lines in Fig. 1 represent the fittings of the numerically obtained $P(s)$ with Eq. (5). The fitted values of β are given in the corresponding panels. This figure shows that the Brody distribution provides very good fittings for the $P(s)$ of the adjacency matrices of ER fully random networks. In fact, the Brody distribution also works well for other complex networks models [33–37].

Now we also construct histograms of $P(s)$ for a large number of values of α to extract systematically the corresponding values of β. Figure 2(a) reports β versus α for five different network sizes. Notice that in all five cases the behavior of β is similar: β shows a smooth transition from zero (the Poisson regime) to one (the Wigner-Dyson or GOE regime) when α increases from $\alpha \ll 1$ (mostly isolated vertices) to one (fully connected networks). Notice also that the larger the network size N, the smaller the value of α needed to approach the GOE limit. This is in fact the reason we observed in Fig. 1 that $P(s)$ is very close to the Wigner-Dyson distribution already for $\alpha = 0.004\,26 \ll 1$.

We recall that the parameter ξ [see Eq. (2)] fixes the density of states of sparse random matrices [11] equivalent to the density of connections in the adjacency matrices we study here. Moreover, ξ was defined as the effective dimension of the sparse random matrix model [11]. Also, Martínez-Mendoza *et al.* [63] showed that scattering and transport properties of tight-binding ER fully random networks are universal for a fixed disorder parameter ξ. Thus, it makes sense to explore the dependence of β on the average degree ξ; in fact, in Fig. 2(b) we show this dependence. We observe that curves for different

[2]It is interesting to mention that Eq. (4), also known as the Wigner surmise, was derived for GOE matrices of size $N = 2$; however, it remarkably provides a very good approximation for the $P(s)$ of GOE matrices with $N \gg 2$.

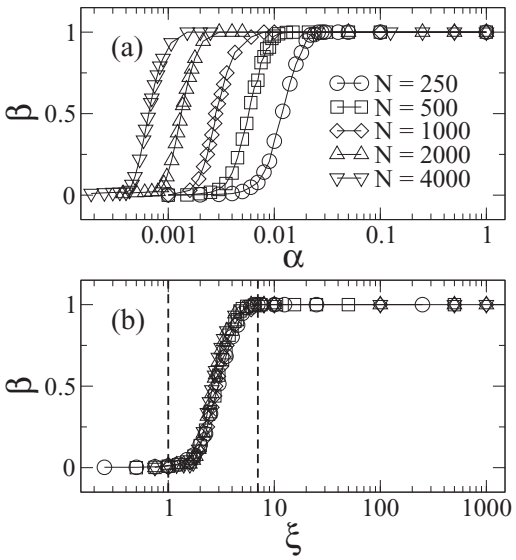

FIG. 2. Brody parameter β as a function of (a) the connectivity α and (b) the average degree $\xi = \alpha N$ for ER fully random networks of sizes ranging from $N = 250$ to 4000. Dashed vertical lines at $\xi = 1$ and 7 mark the onset of the delocalization transition and the onset of the GOE limit, respectively. Error bars are not shown since they are much smaller than the symbol size.

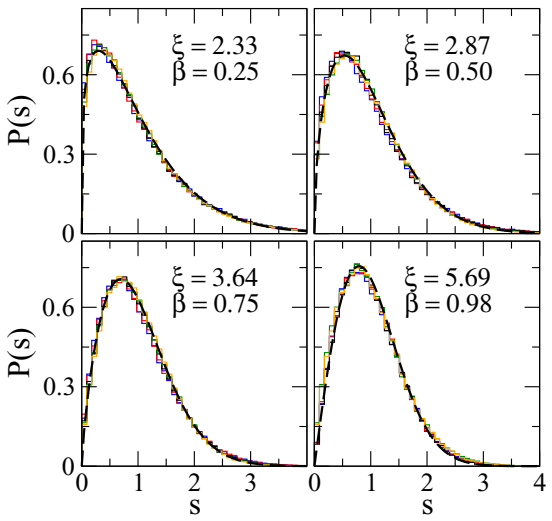

FIG. 3. (Color online) Nearest-neighbor energy-level spacing distribution $P(s)$ for ER fully random networks of sizes ranging from $N = 250$ to 4000 and different values of the average degree ξ (color histograms). Black dashed lines are the Brody distribution of Eq. (5) with $\beta = 0.25$, 0.5, 0.75, and 0.98. Each histogram was computed from 5×10^5 unfolded spacings.

network sizes N fall on top of a universal curve. This means that once ξ is fixed, regardless of the network size, the shape of $P(s)$ is also fixed. We also note that the transition in the form of $P(s)$ takes place in the interval $1 < \xi < 7$; i.e. when $\xi \leqslant 1$ ($\xi \geqslant 7$), $P(s)$ has the Poisson (Wigner-Dyson) shape.

Therefore, we verify the invariance of the form of $P(s)$ for fixed average degree ξ by (i) choosing four representative values of β (0.25, 0.5, 0.75, and 0.98 $\sim$ 1), (ii) extracting the corresponding values of ξ from the universal curve of Fig. 2(b), and (iii) constructing histograms of $P(s)$ for several network sizes for each of the chosen values of ξ. Figure 3 shows that once ξ is fixed, the form of $P(s)$ is invariant. In addition, we include in each panel the corresponding Brody distributions.

Notice that Fig. 2(b) also provides a way to predict the shape of $P(s)$ of ER fully random networks once the average degree ξ is known: When $\xi < 1$, $P(s)$ has the Poisson shape. For $\xi > 7$, $P(s)$ is practically given by the Wigner-Dyson distribution. While in the regime $1 \leqslant \xi \leqslant 7$, $P(s)$ is well described by Brody distributions characterized by a value of $0 < \beta < 1$. Thus, $\xi = 1$ and 7 mark the onset of the delocalization transition and the onset of the GOE limit, respectively.

B. Entropic eigenfunction localization length

In order to characterize quantitatively the complexity of the eigenfunctions of random matrices (and of Hamiltonians corresponding to disordered and quantized chaotic systems) two quantities are mostly used: (i) the information or Shannon entropy and (ii) the eigenfunction participation number. These measures provide the number of principal components of an eigenfunction in a given basis. In fact, both quantities have been already used to characterize the eigenfunctions of the adjacency matrices of random network models (see some examples in Refs. [30,35,38,41,47,52–56,64–67]).

Here we use the Shannon entropy, which for the eigenfunction Ψ^m is given as

$$S = -\sum_{n=1}^{N} \left(\Psi_n^m\right)^2 \ln \left(\Psi_n^m\right)^2. \tag{6}$$

The Shannon entropy S allows us to compute the so-called entropic eigenfunction localization length [68], i.e.,

$$\ell_N = N \exp[-(S_{\mathrm{GOE}} - \langle S \rangle)], \tag{7}$$

where $S_{\mathrm{GOE}} \approx \ln(N/2.07)$ is the entropy of a random eigenfunction with Gaussian distributed amplitudes. We average over all eigenfunctions of an ensemble of adjacency matrices of size N to compute $\langle S \rangle$.[3] With this definition, when $\alpha = 0$, since the eigenfunctions of the adjacency matrices of our random network model have only one nonvanishing component with magnitude equal to one, $\langle S \rangle = 0$ and $\ell_N \approx 2.07$. On the other hand, for $\alpha = 1$, $\langle S \rangle = S_{\mathrm{GOE}}$ and the fully chaotic eigenfunctions extend over the N available vertices in the network, i.e., $\ell_N \approx N$.

Figures 4(a) and 5(a) show $\langle S \rangle / S_{\mathrm{GOE}}$ and ℓ_N / N, respectively, as a function of the connectivity α for the adjacency matrices of ER fully random networks of sizes $N = 500$, 1000, 2000, and 4000. We observe that the curves $\langle S \rangle / S_{\mathrm{GOE}}$ and ℓ_N / N have the same functional form as a function of α. Notice that this behavior is also observed for β in Fig. 2(a). Also these curves are displaced to the left for increasing N. On the other hand, when we plot $\langle S \rangle / S_{\mathrm{GOE}}$ and ℓ_N / N as a function of the average degree ξ, we observe the coalescence of all curves into universal ones [see Figs. 4(b) and 5(b)]. In

[3]We have verified that our observations are not modified when we restrict the averages to a fraction of the eigenfunctions around the band center.

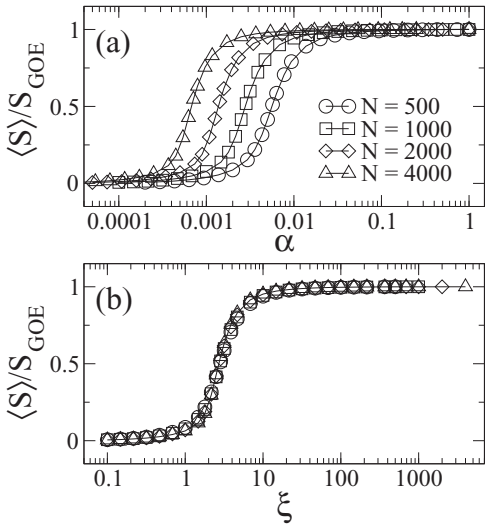

FIG. 4. Average Shannon entropy $\langle S\rangle$ normalized to S_{GOE} as a function of (a) the connectivity α and (b) the average degree ξ for ER fully random networks of sizes ranging from $N = 500$ to 4000. Each point was computed by averaging over 10^6 eigenfunctions.

addition, note that the point at which every ER fully random network becomes globally connected (in the sense that it does not contain isolated subnetworks) $\alpha = (\ln N)/N$ [26] occurs when $\ell_N/N \approx 1/2$ [see the dashed vertical lines in Fig. 5(a)].

From Fig. 5(b) it is clear that the universal behavior of the curve ℓ_N/N as a function of the average degree ξ can be easily described: (i) ℓ_N/N transits from $\approx 2.07/N \sim 0$ to one by moving ξ from zero to N; (ii) for $\xi \lesssim 2$ the eigenfunctions are practically localized since $\ell_N \sim 1$, hence the delocalization transition takes place around $\xi \approx 2$, which is close to previous theoretical and numerical estimations [14–16,22]; and (iii) for

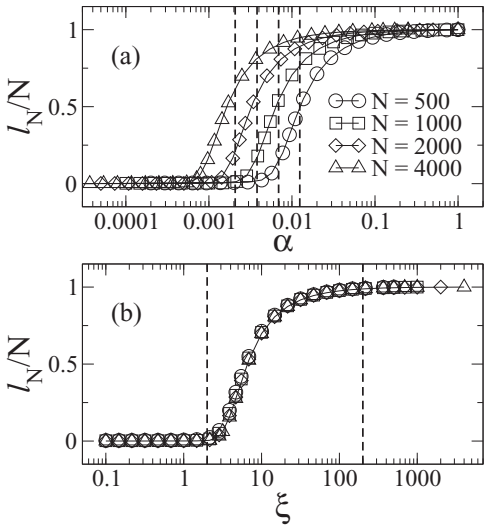

FIG. 5. Entropic eigenfunction localization length ℓ_N normalized to N as a function of (a) the connectivity α and (b) the average degree ξ for ER fully random networks of sizes ranging from $N = 500$ to 4000. Dashed vertical lines in (a) mark the values of $\alpha = (\ln N)/N$ at which every ER fully random network becomes globally connected [26]. Dashed vertical lines in (b) at $\xi = 2$ and $\xi = 200$ mark the onset of the delocalization transition and the onset of the GOE limit, respectively. Each point was computed by averaging over 10^6 eigenfunctions.

$\xi > 200$ the eigenfunctions are practically chaotic and fully extended since $\ell_N \approx N$. Despite the fact that the transition region for ℓ_N/N, which takes place in the range $2 < \xi < 200$, is very large compared to that for β, both quantities are highly correlated and characterize well the Poisson to Wigner-Dyson transition of spectral and eigenfunction properties of the adjacency matrices of ER fully random networks as a function of ξ.

III. OTHER ERDŐS-RÉNYI RANDOM NETWORKS

Notice that with the prescription given above, our ER fully random network model displays maximal disorder, because averaging over the network ensemble implies an average over connectivity and over connection strengths. With this averaging procedure we get rid off any individual network characteristic (such as scars [69], which in turn produce topological resonances [70]) that may lead to deviations from RMT predictions used here as a reference (see also [71]). More specifically, we choose this network model to retrieve well known random matrices in the appropriate limits. (Remember that a diagonal random matrix is obtained for $\alpha = 0$, when the vertices are isolated, whereas a member of the GOE is recovered for $\alpha = 1$, when the network is fully connected.)

However, it is important to add that the maximal disorder we consider above is not necessary for a graph or network to exhibit universal RMT behavior. In fact, it is well known that tight-binding cubic lattices with on-site disorder (known as the three-dimensional Anderson model [4]), forming networks with fixed regular connectivity having very dilute adjacency matrices, show RMT behavior in the metallic phase (see, for example, Refs. [72,73]). Moreover, it has been demonstrated numerically and theoretically that graphs with fixed connectivity show spectral [74,75] and scattering [76,77] universal properties corresponding to RMT predictions. In this case the disorder is introduced either by choosing random bond lengths [74,76,77] (which is a parameter not present in our network model) or by randomizing the vertex-scattering matrices [75] (somehow equivalent to consider random connection strengths). Some of the RMT properties of quantum graphs have already been tested experimentally by the use of small ensembles of small microwave networks with fixed connectivity [78]. Furthermore, complex networks having specific topological properties (such as small-world and scale-free networks, where randomness is applied only to the connectivity) show signatures of RMT behavior in their spectral and eigenfunction properties [33–35,37,47]. Therefore, in the following we search for the scaling properties, if any, of ER-type random networks when the condition of maximal disorder considered above is relaxed.

A. Standard Erdős-Rényi random networks

In the standard ER random network model [8–10], the corresponding adjacency matrices are random matrices with zeros in the main diagonal and ones as nonvanishing off-diagonal elements; i.e., in the adjacency matrix vertices and edges are represented with zeros and ones, respectively [see Eq. (1)]. Even though it has been shown that the $P(s)$ of standard ER random networks is close to the Wigner-Dyson

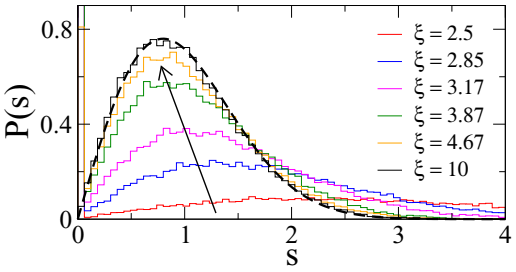

FIG. 6. (Color online) Nearest-neighbor energy-level spacing distribution $P(s)$ for standard ER random networks of size $N = 1000$ and different values of the average degree ξ (color histograms). The black dashed line is the Wigner-Dyson distribution of Eq. (4). The arrow indicates the direction of increasing ξ. Each histogram was computed from 5×10^5 unfolded spacings.

shape for large connectivity ($\alpha \to 1$) [33,34,37], notice that $P(s)$ cannot show the Poisson to Wigner-Dyson transition since in the limit of vanishing connectivity ($\alpha = 0$) the corresponding adjacency matrices are the null matrix.

Figure 6 shows the distribution $P(s)$ for standard ER random networks of size $N = 1000$. We observe that once ξ is large enough, $P(s)$ acquires the expected Wigner-Dyson shape. However, for smaller values of ξ, $P(s)$ develops two components: (i) a prominent peak at $s = 0$ and (ii) a broad part having a local maximum at $s > 0$. The presence of these two components avoids the use of the Brody distribution to describe the shape of $P(s)$ in the transition from isolated vertices to fully connected networks. The same behavior is observed for any other value of N.

It is fair to say that the Brody parameter has already been reported as a function of ξ for standard ER random networks in Ref. [27], however, for $1 \leqslant \xi \leqslant 2.4$ only. The reason to report such a narrow range of ξ is because for vanishing connectivity this model does not approach the Poisson limit and $P(s)$ cannot be fitted by the Brody distribution.

Concerning the Shannon entropy and the entropic eigenfunction localization length for this random network model, we observe, as expected, that $\langle S \rangle / S_{\mathrm{GOE}}$ and ℓ_N/N approach zero when $\alpha \to 0$, whereas they approach one when $\alpha \to 1$. Thus, the delocalization transition of this network model can be well characterized by both $\langle S \rangle$ and ℓ_N. However, there is no universal scaling of $\langle S \rangle / S_{\mathrm{GOE}}$ and ℓ_N/N when plotted as a function of ξ (not shown here).

B. Erdős-Rényi random networks with diagonal disorder

We construct the ER random network model with diagonal disorder by adding self-edges with random strengths such that the corresponding adjacency matrices acquire statistically independent random variables (drawn from a normal distribution with zero mean and variance one) in their main diagonal.[4]

[4]This random network model also corresponds to tight-binding random networks with random on-site potentials and constant (normalized to one) coupling amplitudes between sites, which is in fact the standard prescription for condensed matter models of the Anderson type.

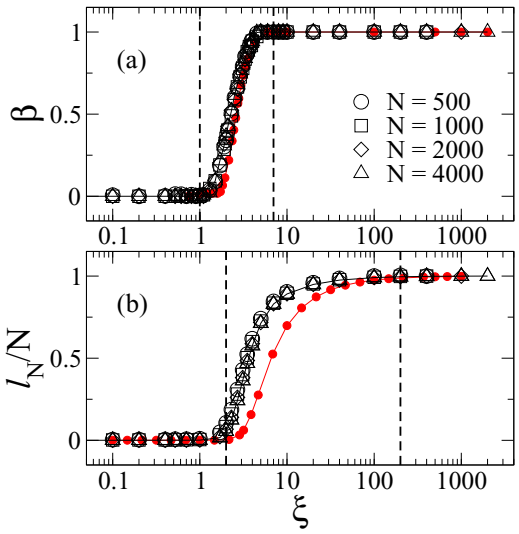

FIG. 7. (Color online) (a) Brody parameter β and (b) entropic eigenfunction localization length ℓ_N (normalized to N) as a function of the average degree ξ for ER random networks with diagonal disorder of sizes ranging from $N = 500$ to 4000. Dashed red vertical lines, displayed for comparison purposes, at $\xi = 1$ and $\xi = 7$ in (a) [at $\xi = 2$ and $\xi = 200$ in (b)] mark the onset of the delocalization transition and the onset of the GOE limit, respectively, of ER fully random networks; see Fig. 2(b) [Fig. 5(b)]. Red data sets corresponding to ER fully random networks of size $N = 4000$ are also included as a reference.

With this construction, we do observe a clear Poisson to Wigner-Dyson transition in the form of $P(s)$ when α moves from zero to one. Moreover, $P(s)$ can be effectively fitted by the Brody distribution (not shown here). Thus, Fig. 7(a) presents the Brody parameter β as a function of the average degree ξ for ER random networks with diagonal disorder. As for ER fully random networks, here we observe that the curves of β vs ξ for different network sizes N fall on top of a universal curve. In addition, we also observe universal behavior for the entropic eigenfunction localization length ℓ_N, normalized to N, as a function of ξ [see Fig. 7(b)]. The delocalization transition in ER networks with diagonal disorder has also been investigated in Ref. [31], but as a function of the disorder strength, by the use of $P(s)$ for networks having $3 \leqslant \xi \leqslant 10$.

It is relevant to add that even though we observe the collapse of the curves β vs ξ and ℓ_N/N vs ξ for ER random networks with diagonal disorder of different sizes, these universal curves are slightly displaced to the left as compared to the corresponding curves for ER fully random networks. More specifically, the onset of the delocalization transition and the onset of the GOE limit occurs for smaller values of ξ in the case of ER random networks with diagonal disorder. See dashed lines and red curves in Fig. 7 (included for comparison purposes), which correspond to ER fully random networks.

IV. SMALL-WORLD NETWORKS

Once we analyzed the universal properties of ER-type random networks, it make sense to further explore other random networks models to look for universal properties. For this task we consider small-world (SW) networks [79].

A SW network, as defined by Watts and Strogatz [79], is constructed by randomly rewiring the edges of a regular ring network consisting of N vertices connected to their $k/2$ nearest neighbors ($k \geqslant 2$ must be an even number).[5] Then, for every vertex, every right-handed edge is reconnected with probability p to a vertex chosen uniformly at random. In the standard SW model multiply connected vertex pairs and self-connections are not allowed. Notice that for $p = 0$ the SW network becomes the original regular ring, whereas for $p = 1$, a random network is obtained where every vertex has a minimum degree of $k/2$.

Notice the following. (i) The parameter k is in fact equivalent to the average degree ξ, given in Eq. (2), which fixes the spectral and eigenfunction properties of ER fully random networks and ER random networks with diagonal disorder. However, k cannot take noninteger values nor values less than 2 as ξ does. Also, it is not an average quantity. (ii) The rewiring probability p is a parameter, independent of k, that drives the SW network model from regular to random. Also, we should stress that as for standard ER random networks, the adjacency matrices of standard SW networks as well have zeros in their main diagonal. This prohibits the use of the Brody distribution to fit the $P(s)$ of standard SW networks when p and k are both small. However, for large p and k, $P(s)$ becomes close to the Wigner-Dyson distribution, as shown in Refs. [33,35,37,49] (for an analytical approach to the spectra of SW networks see Ref. [80]).

Then, as we did in the previous section for ER random networks, here we also consider SW networks with diagonal disorder. That is, we include self-edges having random strengths (drawn from a normal distribution with zero mean and variance one) to each vertex in the network such that the corresponding adjacency matrices exhibit random variables in their main diagonal, whereas the edges joining vertex pairs are still represented by ones in the adjacency matrices. In this way we guarantee that $P(s)$ will have the Poisson shape when p and k are both small. Moreover, we observe (not shown here) that by including diagonal disorder, the Brody distribution fits reasonably well the $P(s)$ of SW networks for any combination of p and k. The delocalization transition in SW networks with diagonal disorder has also been investigated in Ref. [30] as a function of p, N, and disorder strength by the use of the inverse participation ratio of eigenfunctions (equivalent to the entropic eigenfunction localization length we use here); however, the goal there was the implementation of a quantum algorithm able to efficiently simulate the network.

Figure 8 shows the Brody parameter β as a function of p (for several values of k) and k (for several values of p) for SW networks with diagonal disorder of size $N = 1000$. Except for $k = 2$, where $P(s)$ is very close to Poissonian for any p (i.e., $\beta \approx 0$), since the corresponding adjacency matrix is almost diagonal, $P(s)$ shows the transition from Poisson to Wigner-Dyson as a function of p [see Fig. 8(a)]. From this figure we can see that the larger the value of k, the smaller the value of p needed for β to approach one. Notice, for example, that for $k = 20$ the value of $p = 0.001 \ll 1$ makes β very close

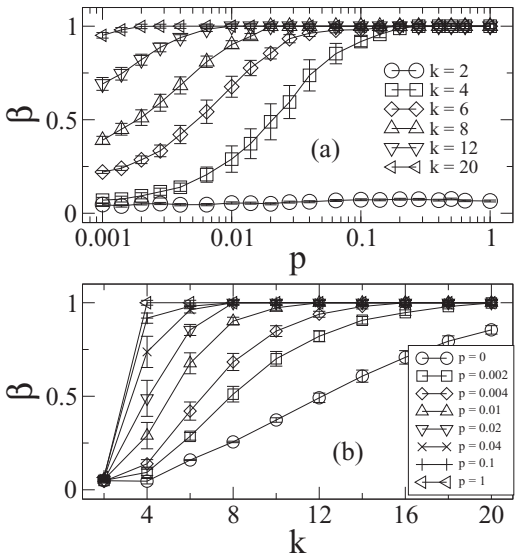

FIG. 8. Brody parameter β as a function of (a) the rewiring probability p and (b) the degree k for SW networks with diagonal disorder of size $N = 1000$.

to one. Clearly, the transition from Poisson to Wigner-Dyson in the form of $P(s)$ is also observed as a function of k for fixed p [see Fig. 8(b)].

Also, in Ref. [33] the Brody parameter was reported as a function of p but for standard SW networks with fixed size $N = 2000$ and average degree $k = 40$. The goal there was to show that β is correlated with two important network parameters: the characteristic path length and the clustering coefficient, quantities that are beyond the scope of our paper. Nevertheless, the delocalization transition was clearly shown as a function of p [analogous to our curves reported in Fig. 8(a) for SW networks with diagonal disorder].

We stress that, in contrast to ER random networks with diagonal disorder, where the average degree ξ fixes their spectral and eigenfunction properties, the degree k does not fix the properties of SW networks with diagonal disorder. This fact is clearly visible in Fig. 9, where we show ℓ_N/N as a function of p for SW networks of four different sizes. Each panel corresponds to a fixed value of degree k where the curves approach each other only when $p > 0.1$.

Finally, we mention that in analogy with the ER fully random networks we studied in Sec. II, here we also considered the case of SW fully random networks; i.e., all nonzero entries of the corresponding adjacency matrices, including the main diagonal, were considered as random variables [in fact, this case has been discussed in Ref. [29] where the transition from Poisson to Wigner-Dyson in the shape of $P(s)$ was reported as a function of p for a network with the fixed parameters $N = 1600$ and $k = 8$]. However, we have not observed a substantial difference from the results reported in Figs. 8 and 9 (not shown here).

V. CONCLUSION

We have studied numerically some spectral and eigenfunction properties of Erdős-Rényi–type random networks, focusing our attention on universality. In particular, we have

[5]Note that when $k = 2$, the ring is a one-dimensional tight-binding ring.

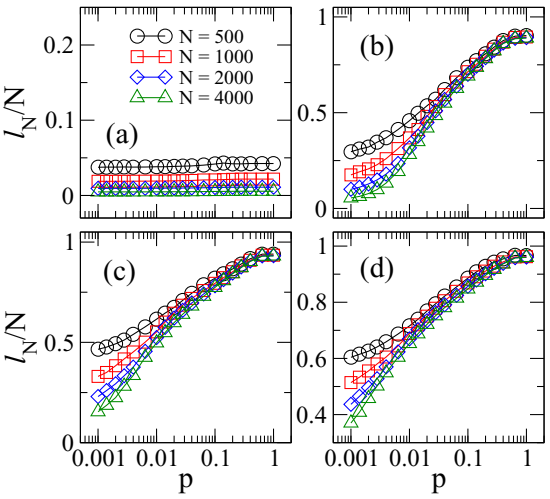

FIG. 9. (Color online) Entropic eigenfunction localization length ℓ_N (normalized to N) as a function of the rewiring probability p for SW networks with diagonal disorder of sizes ranging from $N = 500$ to 4000 for (a) $k = 2$, (b) $k = 8$, (c) $k = 12$, and (d) $k = 20$.

shown for ER fully random networks (where all nonvanishing adjacency matrix elements are Gaussian random variables) and ER networks with diagonal disorder (where the diagonal adjacency matrix elements are Gaussian random variables, whereas the rest of nonvanishing matrix elements are ones) that (i) the nearest-neighbor energy-level spacing distribution $P(s)$, the average Shannon entropy $\langle S\rangle$, and the entropic eigenfunction localization length ℓ_N are universal for fixed average degree $\xi = \alpha N$ (where α and N are the network connectivity and the network size, respectively); (ii) the Brody distribution fits well $P(s)$ in the transition from a Poisson distribution ($\alpha = 0$, isolated vertices) to a Wigner-Dyson distribution ($\alpha = 1$, fully connected network); and (iii) the Brody parameter β as a function of ξ displays an invariant curve.

This analysis provides a way to predict the shape of $P(s)$ of ER-type random networks once the parameter ξ is known. Specifically, for ER fully random networks and ER networks with diagonal disorder we have found that when $0 < \xi < 1$, $P(s)$ is well described by the Poisson shape. This range of ξ values coincides with the regime where a typical ER random graph is composed of isolated trees [26]. We have heuristically located the delocalization transition point around $\xi \approx 1$, in close agreement with the transition value of $\xi \approx 1.4$ reported in Refs. [14–16,22]. Also note that $\xi \approx 3.5$, known as the average degree value at which the diameter of an ER random graph equals the diameter of the giant cluster [26], is located about halfway through the Poisson to Wigner-Dyson transition. Also, we have observed that for $P(s)$ to approach the Wigner-Dyson shape $\xi \geqslant 7$ is needed.

However, we have determined that there is no universal scaling of $\langle S\rangle/S_{\mathrm{GOE}}$ and ℓ_N/N when plotted as a function of ξ for the standard ER model or for SW networks, even though these two quantities describe well the delocalization transition of both models. Moreover, we can affirm that diagonal disorder is needed for a random network model to show the Poisson to Wigner-Dyson transition in the form of $P(s)$.

ACKNOWLEDGMENTS

This work was partially supported by VIEP-BUAP (Grant No. MEBJ-EXC15-I), Fondo Institucional PIFCA (Grant No. BUAP-CA-169), and CONACyT (Grants No. I0010-2014-246246 and No. CB-2013-220624). F.A.R. acknowledges CNPq (Grant No. 305940/2010-4), FAPESP (Grants No. 2011/50761-2 and No. 2013/26416-9), and NAP eScience-PRP-USP for financial support. T.K.D.P. would like to acknowledge FAPESP (Grant No. 2012/22160-7) for support through the scholarship provided.

[1] L. da F. Costa, O. N. Oliveira, Jr., G. Travieso, F. A. Rodrigues, P. R. Villas Boas, L. Antiqueira, M. P. Viana, and L. E. C. Rocha, Adv. Phys. **60**, 329 (2011).
[2] A. L. Barabási, Philos. Trans. R. Soc. London Ser. A **371**, 20120375 (2013).
[3] M. E. J. Newman, *Networks: An Introduction* (Oxford University Press, New York, 2010).
[4] P. W. Anderson, Phys. Rev. **109**, 1492 (1958).
[5] O. Mülken and A. Blumen, Phys. Rep. **502**, 37 (2011).
[6] S. Boccaletti, V. Latora, Y. Moreno, M. Chavez, and D.-U. Hwang, Phys. Rep. **424**, 175 (2006).
[7] B. Bollobás, *Modern Graph Theory* (Springer, New York, 1998), Vol. 184, pp. 215–252.
[8] R. Solomonoff and A. Rapoport, Bull. Math. Biophys. **13**, 107 (1951).
[9] P. Erdős and A. Rényi, Publ. Math. (Debrecen) **6**, 290 (1959).
[10] P. Erdős and A. Rényi, Publ. Math. Inst. Hungarian Acad. Sci. **5**, 17 (1960); Acta Math. Sci. Hungary **12**, 261 (1961).
[11] A. D. Jackson, C. Mejia-Monasterio, T. Rupp, M. Saltzer, and T. Wilke, Nucl. Phys. A **687**, 405 (2001).
[12] G. J. Rodgers and A. J. Bray, Phys. Rev. B **37**, 3557 (1988).
[13] G. Rodgers and C. de Dominicis, J. Phys. A: Math. Gen. **23**, 1567 (1990).
[14] S. N. Evangelou and E. N. Economou, Phys. Rev. Lett. **68**, 361 (1992).
[15] A. D. Mirlin and Y. V. Fyodorov, J. Phys. A: Math. Gen. **24**, 2273 (1991).
[16] S. N. Evangelou, J. Stat. Phys. **69**, 361 (1992).
[17] G. Semerjian and L. F. Cugliandolo, J. Phys. A: Math. Gen. **35**, 4837 (2002).
[18] A. Khorunzhy and G. J. Rodgers, J. Math. Phys. **38**, 3300 (1997).
[19] R. Kühn, J. Phys. A: Math. Gen. **41**, 295002 (2008).
[20] T. Rogers, I. P. Castillo, R. Kühn, and K. Takeda, Phys. Rev. E **78**, 031116 (2008).
[21] F. Slanina, Phys. Rev. E **83**, 011118 (2011).

[22] Y. V. Fyodorov and A. D. Mirlin, Phys. Rev. Lett. **67**, 2049 (1991).

[23] Y. Kabashima, H. Takahashi, and O. Watanabe, J. Phys.: Conf. Ser. **233**, 012001 (2010); Y. Kabashima and H. Takahashi, J. Phys. A: Math. Gen. **45**, 325001 (2012).

[24] T. Rogers and I. P. Castillo, Phys. Rev. E **79**, 012101 (2009); I. Neri and F. L. Metz, Phys. Rev. Lett. **109**, 030602 (2012).

[25] R. Fossion, G. Torres-Vargas, S. Díaz-Gómez, and J. C. López Vieyra, arXiv:1402.6786.

[26] R. Albert and A. L. Barabási, Rev. Mod. Phys. **74**, 47 (2002).

[27] G. Palla and G. Vattay, New J. Phys. **8**, 307 (2006).

[28] B. Derrida and G. J. Rodgers, J. Phys. A: Math. Gen. **26**, L457 (1993).

[29] C. P. Zhu and S. J. Xiong, Phys. Rev. B **62**, 14780 (2000).

[30] O. Giraud, B. Georgeot, and D. L. Shepelyansky, Phys. Rev. E **72**, 036203 (2005).

[31] M. Sade, T. Kalisky, S. Havlin, and R. Berkovits, Phys. Rev. E **72**, 066123 (2005).

[32] L. Jahnke, J. W. Kantelhardt, R. Berkovits, and S. Havlin, Phys. Rev. Lett. **101**, 175702 (2008).

[33] J. N. Bandyopadhyay and S. Jalan, Phys. Rev. E **76**, 026109 (2007).

[34] S. Jalan and J. N. Bandyopadhyay, Physica A **387**, 667 (2008).

[35] G. Zhu, H. Yang, C. Yin, and B. Li, Phys. Rev. E **77**, 066113 (2008).

[36] S. Jalan, Phys. Rev. E **80**, 046101 (2009).

[37] S. Jalan and J. N. Bandyopadhyay, Phys. Rev. E **76**, 046107 (2007).

[38] L. Gong and P. Tong, Phys. Rev. E **74**, 056103 (2006).

[39] C. P. Zhu and S. J. Xiong, Phys. Rev. B **63**, 193405 (2001).

[40] K. I. Goh, B. Kahng, and D. Kim, Phys. Rev. E **64**, 051903 (2001).

[41] I. J. Farkas, I. Derényi, A. L. Barabási, and T. Vicsek, Phys. Rev. E **64**, 026704 (2001).

[42] I. Farkas, I. Derényi, H. Jeong, Z. Néda, Z. N. Oltvai, E. Ravasz, A. Schubert, A. L. Barabási, and T. Vicsek, Physica A **314**, 25 (2002).

[43] S. N. Dorogovtsev, A. V. Goltsev, J. F. F. Mendes, and A. N. Samukhin, Phys. Rev. E **68**, 046109 (2003); Physica A **338**, 76 (2004).

[44] R. F. S. Andrade and J. G. V. Miranda, Physica A **356**, 1 (2005).

[45] C. Kamp and K. Christensen, Phys. Rev. E **71**, 041911 (2005).

[46] G. J. Rodgers, K. Austin, B. Kahng, and D. Kim, J. Phys. A: Math. Gen. **38**, 9431 (2005).

[47] O. Mülken, V. Pernice, and A. Blumen, Phys. Rev. E **76**, 051125 (2007).

[48] T. Nagao and G. J. Rodgers, J. Phys. A: Math. Theor. **41**, 265002 (2008).

[49] S. Jalan and J. N. Bandyopadhyay, Europhys. Lett. **87**, 48010 (2009).

[50] G. Ergün and R. Kühn, J. Phys. A: Math. Theor. **42**, 395001 (2009); R. Kühn and J. van Mourik, *ibid.* **44**, 165205 (2011).

[51] J. X. de Carvalho, S. Jalan, and M. S. Hussein, Phys. Rev. E **79**, 056222 (2009).

[52] A. L. Cardoso, R. F. S. Andrade, and A. M. C. Souza, Phys. Rev. B **78**, 214202 (2008).

[53] O. Giraud, B. Georgeot, and D. L. Shepelyansky, Phys. Rev. E **80**, 026107 (2009); B. Georgeot, O. Giraud, and D. L. Shepelyansky, *ibid.* **81**, 056109 (2010).

[54] S. Jalan, N. Solymosi, G. Vattay, and B. Li, Phys. Rev. E **81**, 046118 (2010).

[55] S. Jalan, G. Zhu, and B. Li, Phys. Rev. E **84**, 046107 (2011).

[56] F. Slanina, Eur. Phys. J. B **85**, 361 (2012).

[57] M. L. Metha, *Random Matrices* (Elsevier, Amsterdam, 2004).

[58] F. Haake, *Quantum Signatures of Chaos* (Springer, Berlin, 2010).

[59] T. A. Brody, Lett. Nuovo Cimento **7**, 482 (1973).

[60] T. A. Brody, J. Flores, J. B. French, P. A. Mello, A. Pandey, and S. S. M. Wong, Rev. Mod. Phys. **53**, 385 (1981).

[61] As examples of representative systems characterized by the Brody distribution we mention many-body systems [R. Modak and S. Mukerjee, New J. Phys. **16**, 093016 (2014)]; mixed-chaotic billiards [B. Batistic and M. Robnik, J. Phys. A: Math. Theor. **46**, 315102 (2013)]; the kicked rotator [B. Batistic, T. Manos, and M. Robnik, Europhys. Lett. **102**, 50008 (2013)]; random matrix ensembles [G. LeCaër, C. Male, and R. Delannay, Physica A **383**, 190 (2007)]; and biological systems [R. Potestio, F. Caccioli, and P. Vivo, Phys. Rev. Lett. **103**, 268101 (2009)]. In fact, the Brody distribution was recently generalized to include also the Gaussian unitary ensemble limit in H. Sabri, S. S. Hashemi, B. R. Maleki, and M. A. Jafarizadeh, Random Matrices: Theor. Appl. **03**, 1450017 (2014).

[62] Indeed, in J. Sakhr and J. M. Nieminen, Phys. Rev. E **72**, 045204(R) (2005), it was shown that in the nearest-neighbor spacing distribution of random points uniformly distributed on a self-similar fractal space the Brody parameter corresponds to the fractal dimension.

[63] A. J. Martínez-Mendoza, A. Alcazar-López, and J. A. Méndez-Bermúdez, Phys. Rev. E **88**, 012126 (2013).

[64] F. Passerini and S. Severini, arXiv:0812.2597v2.

[65] G. D. Paparo, M. Müller, F. Comellas, and M. A. Martin-Delgado, Sci. Rep. **3**, 2773 (2013).

[66] G. Menichetti, D. Remondini, P. Panzarasa, R. J. Mondragón, and G. Bianconi, PLoS ONE **9**, e97857 (2014).

[67] T. Martin, X. Zhang, and M. E. J. Newman, Phys. Rev. E **90**, 052808 (2014).

[68] F. M. Izrailev, Phys. Rep. **196**, 299 (1990).

[69] H. Schanz and T. Kottos, Phys. Rev. Lett. **90**, 234101 (2003).

[70] S. Gnutzmann, H. Schanz, and U. Smilansky, Phys. Rev. Lett. **110**, 094101 (2013).

[71] T. K. DM. Peron, P. Ji, F. A. Rodrigues, and J. Kurths, arXiv:1310.3389.

[72] B. I. Shklovskii, B. Shapiro, B. R. Sears, P. Lambrianides, and H. B. Shore, Phys. Rev. B **47**, 11487 (1993).

[73] B. L. Altshuler, V. E. Kravtsov, and I. V. Lerner, in *Mesoscopic Phenomena in Solids*, edited by B. L. Altshuler, P. A. Lee, and R. A. Webb (North-Holland, Amsterdam, 1991); in *Mesoscopic Quantum Physics*, edited by E. Akkermans, G. Montambaux, J.-L. Pichard, and J. Zinn-Justin, Proceedings of the Les Houches Summer School of Theoretical Physics, LXI (North-Holland, Amsterdam, 1995); K. B. Efetov, *Supersymmetry in Disorder and Chaos* (Cambridge University Press, Cambridge, 1997).

[74] T. Kottos and U. Smilansky, Phys. Rev. Lett. **79**, 4794 (1997); Ann. Phys. (NY) **273**, 1 (1999); S. Gnutzmann and A. Altland, Phys. Rev. Lett. **93**, 194101 (2004); Phys. Rev. E **72**, 056215 (2005); S. Gnutzmann and U. Smilansky, Adv. Phys. **55**, 527 (2006).

[75] T. Kottos and H. Schanz, Physica E **9**, 523 (2001).

[76] T. Kottos and U. Smilansky, Phys. Rev. Lett. **85**, 968 (2000); J. Phys. A **36**, 3501 (2003).
[77] Z. Pluhar and H. A. Weidenmüller, Phys. Rev. Lett. **110**, 034101 (2013).
[78] O. Hul, S. Bauch, P. Pakonski, N. Savytskyy, K. Zyczkowski, and L. Sirko, Phys. Rev. E **69**, 056205 (2004); M. Lawniczak, O. Hul, S. Bauch, P. Seba, and L. Sirko, *ibid.* **77**, 056210 (2008); M. Lawniczak, S. Bauch, O. Hul, and L. Sirko, *ibid.* **81**, 046204 (2010).
[79] D. J. Watts and S. H. Strogatz, Nature (London) **393**, 440 (1998).
[80] C. Grabow, S. Grosskinsky, and M. Timme, Phys. Rev. Lett. **108**, 218701 (2012).